Journal of Advances in Manufacturing Engineering
Web page info: https://eds.yildiz.edu.tr/JAME
DOI: 10.14744/ytu.jame.2021.00003

Original Article

Weibull distribution of selective laser melted AlSi10Mg parts for compression testing

Hamaid Mahmood KHAN[1,*], Mehmet Hüsnü DİRİKOLU[2], Ebubekir KOÇ[1]

[1]*Aluminum Test Training and Research Centre, Fatih Sultan Mehmet Vakıf University, İstanbul, Turkey*
[2]*Department of Mechanical Engineering, İstanbul University Faculty of Engineering, İstanbul, Turkey*

ARTICLE INFO

Article history
Received: 15 February 2021
Accepted: 03 April 2021

Key words:
AlSi10Mg, compression testing, selective laser sintering, weibull distribution.

ABSTRACT

Selective laser melting (SLM) is an additive manufacturing process to fabricate three-dimensional structures by fusing powder particles using a computer-guided laser source. The SLM process can produce lightweight bespoke designs, having high strength comparable to conventional components. However, the developed surface texture and some of the mechanical properties are still sub-standard compared to the conventional components. The process uncertainty can produce inconsistency in parts' properties, even those prepared concurrently, affecting SLM parts' repeatability and quality. Therefore, designing applications based on the most probable outcome of the desired properties can embrace process uncertainty. Weibull distribution is a statistical-based probability distribution method that measures the likelihood of the values' occurrence of any random variable falling in a specific set of values. In this study, the Weibull distribution measured the relative likelihood (90% probability) of the compressive yield, and ultimate strength of the SLM prepared AlSi10Mg samples in a given 22 random sample size. The results showed that the compressive yield and ultimate strength fall between 321 MPa to 382 MPa and 665 MPa to 883 MPa.

Cite this article as: Khan HM, Dirikolu MH, Koç E. Weibull distribution of selective laser melted AlSi10Mg parts for compression testing. J. Adv. Manuf. Eng. 2021;2:1:14–19.

INTRODUCTION

Selective laser melting (SLM) is a powder-based additive manufacturing (AM) process where a high-power laser source melts discrete powder particles to form solid components [1]. The toolless production, design freedom, low fabrication cost, and less material waste are some unique advantages of the selective laser melting process over conventional ones [2, 3]. SLM enables the fabrication of complex topologies with design porosity that is nearly impossible using conventional routes [4]. The mechanical properties of SLM components are either superior or comparable to conventional structures [1, 5]. However, high surface roughness, sub-surface porosity, high residu-

***Corresponding author.**
*E-mail address: hamaid.khan@gmail.com

This paper was presented at the Additive manufacturing conference, Turkey in İstanbul, Turkey (AMC Turkey, 2019), on 17–18 October 2019.

al stress, and non-equilibrium microstructure can produce unwanted mechanical properties in SLM components that may limit their wide commercial acceptance [6–8]. These unacceptable mechanical effects are the results of process uncertainties. A fresh compact layer of powder particles is essential for near-net-shape part fabrication [9]. However, uncertainty in powder morphology and unoptimized processing conditions can lead to variability in structural porosity. SLM components with high structural porosity result in low mechanical strength [10, 11]. The SLM processing parameters, such as laser power, scan speed, scan spacing, and layer thickness, are critical to the final mechanical properties of SLM components. Optimizing laser parameters can help attain the near-net-shape structure with limited structural porosity. The laser parameters can be optimized using a trial and error approach. However, optimizing powder distribution in the powder bed is still farfetched [1, 12, 13].

The uncertainties in powder granulometry within the build chamber, such as powder size, shape, distribution, and powder packing density, can significantly alter final mechanical and surface properties, hindering parts' repeatability and product quality [5, 14, 15]. Moreover, the processing conditions such as the scanning location, geometry type, and atmospheric conditions can alter the final mechanical properties of the SLM components [16, 17]. Therefore, the mechanical properties of SLM components fabricated with identical laser parameters can still have different surface roughness, density, and mechanical strength. Currently, it is challenging to control material parameters and SLM processing conditions; therefore, the changes in mechanical properties are inevitable. It is, therefore, essential to statistically investigate a large sample size to measure the deviation in mechanical properties and to identify the most probable outcome of these properties for the final part design. In this paper, we used a Weibull distribution method to measure the statistical distribution of compressive strength of SLM prepared AlSi10Mg samples. The continuous probability distribution functions like the Weibull distribution are suitable to measure the probability of the occurrence of different outcomes in an experiment [18]. Several works have reported using the Weibull distribution function to determine mechanical properties for composite materials [19, 20]. In additive manufacturing, E. Brandl et al. [21] used Weibull distribution to interpolate Wohler curves to investigate the fatigue strength in post-heat-treated samples built in different directions. It is often helpful in industrial engineering, reliability engineering, and failure analysis [20, 22]. In this work, we measured the compressive yield and ultimate strength of 22 samples of the SLM prepared AlSi10Mg material. Later, the Weibull distribution functions were used to measure the variation in the compressive stress values, and the results are presented in graphical forms.

MATERIAL AND METHODS

Gas atomized maraging steel powder (EOS GmbH) with an average diameter of 40µm was used to fabricate the SLM samples. Table 1 shows the laser processing parameters used in the fabrication of AlSi10Mg compression samples (Fig. 1). SLM M290 (EOS Group) 3D printing machine characterized by a single Yttrium fiber laser and a build chamber of size 252x252x325 mm^3 is used to fabricate additive samples. The entire process was carried out in the presence of pure argon gas. The oxygen level was maintained below 10000 ppm with the help of an oxygen analyzer. Herein, all the rectangular prismatic samples of size 5x5x5 mm^3 were fabricated simultaneously in a horizontal direction using a 67° rotational scanning strategy. The samples were separated from the platform bed after fabrication, and later support structures were removed for further processing. Prior to the compression test, the samples' surfaces were polished and their sizes were measured for statistical evaluation. The compression testing was carried out as per the ASTM E 8M-04 standard on an Instron 5982 dual column testing system with a 100 kN loading capacity.

The downward speed of 0.5mm/min was used amid room conditions during the compression tests. Table 2 lists down the compressive yield stress (0.2% offset) values for all the samples.

RESULTS AND DISCUSSION

Weibull Distribution

Weibull distribution is used to measure the characteristic compression stress values of SLM processed samples.

Table 1. Processing parameters and physical values of AlSi10Mg

Properties	Values
Laser power	370 W
Scanning rate	1300 mm/s
Hatching	190 µm
Layer thickness	30 µm
Spot size diameter	100 µm
Scanning strategy	Alternate, 67^0

Figure 1. Additively manufactured 22 samples of AlSi10Mg.

Table 2. Measured compressive yield stress and strength

S. No:	Compressive Yield Stress (MPa)	Compressive Strength (MPa)	Dimension (mm^2) (L x W)	Area (mm^2)
1	329.89	585.06	5.11 x 5.14	26.27
2	353.02	585.69	5.10 x 5.11	26.06
3	321.03	561.83	5.09 x 5.08	25.86
4	382.59	571.90	5.12 x 5.11	26.16
5	337.52	578.68	5.11 x 5.11	26.11
6	344.01	579.87	5.11 x 5.09	26.01
7	342.98	586.90	5.11 x 5.11	26.11
8	359.96	566.04	5.16 x 5.11	26.37
9	337.67	579.67	5.12 x 5.10	26.11
10	368.35	588.66	5.12 x 5.11	26.16
11	364.12	598.93	5.11 x 5.10	26.06
12	361.77	618.11	5.09 x 5.08	25.86
13	356.18	594.29	5.09 x 5.09	26.11
14	349.61	592.75	5.11 x 5.11	25.91
15	335.77	590.89	5.12 x 5.11	26.11
16	344.34	574.45	5.11 x 5.12	26.16
17	354.14	573.43	5.12 x 5.12	26.16
18	340.27	582.35	5.15 x 5.12	26.21
19	341.72	592.90	5.12 x 5.09	26.37
20	338.02	592.65	5.14 x 5.12	26.06
21	370.92	593.38	5.12 x 5.11	26.32
22	343.79	592.50	5.11 x 5.11	26.16

Out of the two popular forms, the three-parameter Weibull distribution is given by [23];

$$F(x;\alpha,\beta,\gamma) = 1 - \exp\left(-\left(\frac{x-\alpha}{\beta}\right)^{\gamma}\right), \quad (1)$$

α,β,γ≥0,

Where, α, β, and γ are location, scale, and shape parameters, respectively. If α=0, the three-parameter transforms into two-parameter Weibull distribution function;

$$F(x;\beta,\gamma) = 1 - \exp\left(-\left(\frac{x}{\beta}\right)^{\gamma}\right), \quad (2)$$

β,γ≥0,

The probability function F(x;β,γ) represents that compressive strength is equal to or less than the value x. There is another term reliability R(x;β,γ) that can be inferred from the equality F(x;β,γ)+ R(x;β,γ)=1. Here, R(x;β,γ) represents the probability of compressive strength is at least equal to x.

$$R(x;\beta,\gamma) = \exp\left(-\left(\frac{x}{\beta}\right)^{\gamma}\right), \quad (3)$$

β,γ≥0,

To evaluate the scale β, and shape γ parameters of the distribution function F(x;β,γ)A method of linear regression is applied where a straight line is fitted using MS Excel™ software.

Linear regression method

Using double logarithm, equation $F(x;\beta,\gamma) = 1 - \exp\left(-\left(\frac{x}{\beta}\right)^{\gamma}\right)$ is transformed into a straight-line form for easy evaluation.

$$\ln\left[\ln\left(\frac{1}{1-F(x;\beta,\gamma)}\right)\right] = \gamma\ln(x) - \gamma\ln(\beta), \quad (4)$$

Equation 4 resembles a straight line Y=mX+c. The function F(x;β,γ) can be estimated from the observed compression values ordered in an increasing sequence. The function F(x;β,γ) is determined as;

$$F(x_i;\beta,\gamma) = (x_i - 0.5)/n, \quad (5)$$

Where n=22 is the total number of samples. The values $Y = \ln\left[\ln\left(\frac{1}{1-F(x;\beta,\gamma)}\right)\right]$ and $X = \ln(x)$ are plotted for linear regression to estimate the parameters β and γ as shown in Figure 2. The equation thus obtained is;

Y=28.265X-166.04,

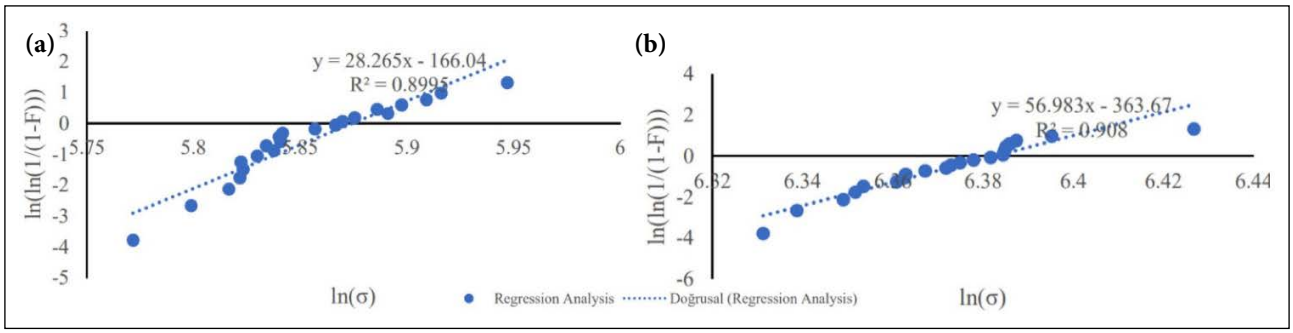

Figure 2. The regression line for **(a)** compressive yield stress and **(b)** compressive strength.

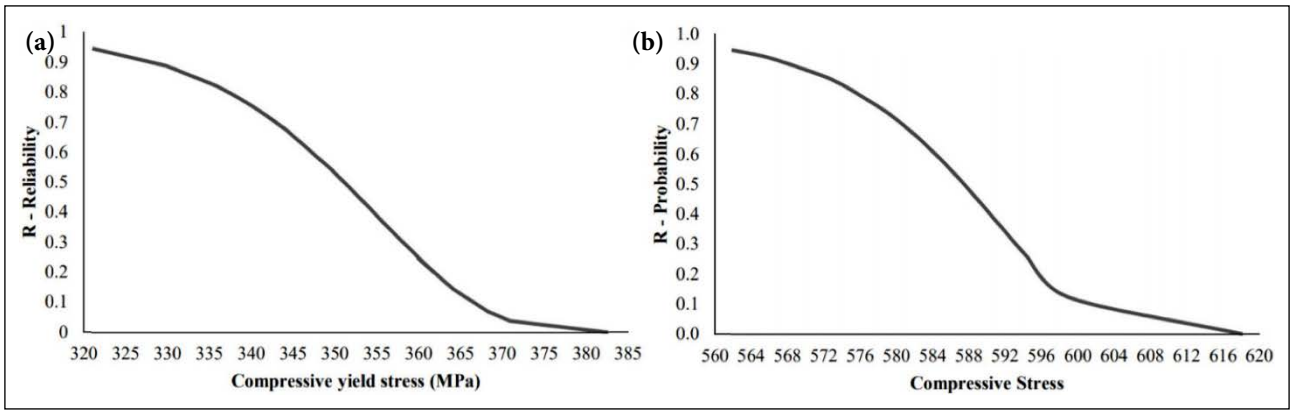

Figure 3. Weibull reliability distribution for **(a)** yield stress and **(b)** compressive strength.

Here, m=γ=28.265 is the slope of the regression line. The shape parameter γ>0 specifies an increasing failure rate due to compressive loading. Larger γ signifies the higher possibility of a material fracture for every unit increase in compression values. Parameter β measures the distribution scale of the data, and it can be obtained from equations 4 and 6. As a result, we found β=355.73 MPa. The reliability R(x;β,γ) for compression stress, x=355.73MPa was measured 0.3545, which is 35.45% of the tested samples have the compressive yield strength of at least 355.73 MPa. A plot of R(x;β,γ) is shown in Figure 3. The plot shows that 90% of the component with a compressive yield strength of about 328.08 MPa will not yield under compression loading. Table 3 lists the other essential values corresponding to yield and compressive strength.

Table 2 shows that the SLM prepared ALSi10Mg components exhibit different compressive yields and ultimate strength. The compressive yield strength and the ultimate compressive strength of SLM samples were found to vary in between 321–382 MPa and 561–618 MPa, respectively, which agrees well with previous results [24, 25]. The difference of approximately 60 MPa in the compressive yield and ultimate strength is pretty significant for SLM AlSi10Mg samples. The change in part's porosity arising from the process uncertainty can be the reason for such a massive difference in SLM samples' compression values. The structural porosity is generally high in SLM structures, and the variability can further increase depending on the part location. The change in

Table 3. Reliability distributions corresponding to various stress values for both compressive yield stress and compressive strength

Parameters Equation		Compressive yield strength		Compressive strength	
		y=28.265x-166.04		y=17.024x-113.71	
m=γ		28.265		17.024	
β		355.73		795.65	
R(x;β,γ)	@x	355.73	35.45%	591.20	36.74%
Lower limit, R		321.03	94.65%	561.83	94.66%
Upper limit, R		382.5	0.04%	618.11	~0.00%
R=90%		328.08 MPa		569.07 MPa	

surface roughness and mechanical strength due to part position in the powder bed has been discussed previously in the literature [1, 5, 16].

Since the samples were developed at optimized laser parameters provided by machine (EOS) suppliers, there are limited chances to improve the overall mechanical properties by choosing other optimized processing parameters. Since we know, SLM offers a wide processing window for part fabrication, and several parameter sets can help achieve near-net-shape components [1, 26]. Therefore, the only way to improve SLM components' mechanical properties is through post-processing techniques, albeit they are time-consuming and add additional cost to production. For the as-printed structures, this study clearly shows that samples' property in the SLM build chamber is not stable. Several factors can produce a massive change in the final mechanical properties. Therefore, before designing components in SLM machines, the variability in mechanical properties should be considered. Failing to do so can produce a significant change in part's performance, even leading to component failure.

CONCLUSION

AlSi10Mg is one of the most tested alloys in the SLM process, and it is extensively used in the production of several components in automobiles, aircraft, and other industrial sectors. Weibull distribution was used to measure the compressive yield and ultimate strength of the tested 22 specimens of AlSi10Mg to obtain the processed parts' reliability to withstand the variable compression loading. In the present case, the compressive yield strength and the compressive strength of the tested specimens with 90% reliability were found to be 328.08 MPa and 569.07 MPa, respectively.

Data Availability Statement

All graphs and data obtained or generated during the investigation appear in the published article.

Author's Contributions

Hamaid Mahmood Khan: conceived the investigation, oversaw the course of the experiment, and developed and authored the text.

Mehmet Hüsnü Dirikolu: Conceptualized the study, drafted, supervised, and assisted in writing the manuscript.

Ebubekir Koç: Drafted, supervised, and assisted in writing the manuscript.

Conflict of interest

The authors declared no potential conflicts of interest with respect to the research, authorship, and/or publication of this article.

Ethics

There are no ethical issues with the publication of this manuscript.

REFERENCES

[1] Khan, H. M., Karabulut, Y., Kitay, O., Kaynak, Y., Jawahir, I. S., Mahmood, K. H., … Jawahir, I. S. (2021). Influence of the post-processing operations on surface integrity of metal components produced by laser powder bed fusion additive manufacturing: a review. Machining Science and Technology, 25(1), 118–176. https://doi.org/10.1080/10910344.2020.1855649

[2] Ahmadi, A., Mirzaeifar, R., Moghaddam, N. S., Turabi, A. S., Karaca, H. E., and Elahinia, M. (2016). Effect of manufacturing parameters on mechanical properties of 316L stainless steel parts fabricated by selective laser melting: A computational framework. Materials and Design, 112, 328–338. https://doi.org/10.1016/j.matdes.2016.09.043

[3] Brandão, A. D., Gumpinger, J., Gschweitl, M., Seyfert, C., Hofbauer, P., and Ghidini, T. (2017). Fatigue Properties of Additively Manufactured AlSi10Mg-Surface Treatment Effect. In Procedia Structural Integrity (Vol. 7, pp. 58–66). https://doi.org/10.1016/j.prostr.2017.11.061

[4] Plocher, J., and Panesar, A. (2019). Review on design and structural optimisation in additive manufacturing: Towards next-generation lightweight structures. Materials and Design. Elsevier Ltd. https://doi.org/10.1016/j.matdes.2019.108164

[5] DebRoy, T., Wei, H. L., Zuback, J. S., Mukherjee, T., Elmer, J. W., Milewski, J. O., … Zhang, W. (2018). Additive manufacturing of metallic components – Process, structure and properties. Progress in Materials Science, 92, 112–224. https://doi.org/10.1016/j.pmatsci.2017.10.001

[6] Everton, S. K., Hirsch, M., Stravroulakis, P., Leach, R. K., and Clare, A. T. (2016). Review of in-situ process monitoring and in-situ metrology for metal additive manufacturing. Materials and Design, 95, 431–445. https://doi.org/10.1016/j.matdes.2016.01.099

[7] Patterson, A. E., Messimer, S. L., and Farrington, P. A. (2017). Overhanging Features and the SLM/DMLS Residual Stresses Problem: Review and Future Research Need. Technologies, 5(2), 15. https://doi.org/10.3390/technologies5020015

[8] Khan, H. M., Dirikolu, M. H., and Koç, E. (2018). Parameters optimization for horizontally built circular profiles: Numerical and experimental investigation. Optik, 174(August), 521–529. https://doi.org/10.1016/j.ijleo.2018.08.095

[9] Olakanmi, E. O., Cochrane, R. F., and Dalgarno, K. W. (2015). A review on selective laser sintering/melting (SLS/SLM) of aluminium alloy powders: Processing, microstructure, and properties. Progress in Materials Science, 74, 401–477. https://doi.org/10.1016/j.pmatsci.2015.03.002

[10] Fiegl, T., Franke, M., and Körner, C. (2019). Impact of build envelope on the properties of additive manufactured parts from AlSi10Mg. Optics and Laser Technology, 111(September 2018), 51–57. https://doi.org/10.1016/j.optlastec.2018.08.050

[11] Wang, X., Xu, S., Zhou, S., Xu, W., Leary, M., Choong, P., … Xie, Y. M. (2016). Topological design and additive manufacturing of porous metals for bone scaffolds and orthopaedic implants: A review. Biomaterials. Elsevier Ltd. https://doi.org/10.1016/j.biomaterials.2016.01.012

[12] Khan, H. M., Sirin, T. B., Tarakci, G., Bulduk, M. E., Coskun, M., Koc, E., and Kaynak, Y. (2021). Improving the surface quality and mechanical properties of selective laser sintered PA2200 components by the vibratory surface finishing process. SN Applied Sciences.

[13] Liu, Y., Zhang, J., Yang, Y., Li, J., and Chen, J. (2017). Study on the influence of process parameters on the clearance feature in non-assembly mechanism manufactured by selective laser melting. Journal of Manufacturing Processes, 27, 98–107. https://doi.org/10.1016/j.jmapro.2017.04.005

[14] Upadhyay, M., Sivarupan, T., and El Mansori, M. (2017). 3D printing for rapid sand casting—A review. Journal of Manufacturing Processes, 29, 211–220. https://doi.org/10.1016/j.jmapro.2017.07.017

[15] Sander, G., Tan, J., Balan, P., Gharbi, O., Feenstra, D. R., Singer, L., … Birbilis, N. (2018). Corrosion of additively manufactured alloys: A review. Corrosion, 74(12), 1318–1350. https://doi.org/10.5006/2926

[16] Öter, Z. Ç., Coşkun, M., and Ebubekir, K. (2018). Effect of Building Platform Position on the Surface Quality, Dimensional Accuracy, and Geometrical Precision of Direct Metal Laser Sintering (DMLS) Parts, (October), 1–5.

[17] Oter, Z. C. Z. C., Coskun, M., Akca, Y., Surmen, O., Yilmaz, M. S., Ozer, G., … Koc, E. (2019). Support optimization for overhanging parts in direct metal laser sintering. Optik, 181(November 2018), 575–581. https://doi.org/10.1016/j.ijleo.2018.12.072

[18] Keleş, Ö., Blevins, C. W., and Bowman, K. J. (2017). Effect of build orientation on the mechanical reliability of 3D printed ABS. Rapid Prototyping Journal, 23(2), 320–328. https://doi.org/10.1108/RPJ-09-2015-0122

[19] Birgoren, B., and Dirikolu, M. H. (2004). A computer simulation for estimating lower bound fracture strength of composites using Weibull distribution. Composites Part B: Engineering, 35(3), 263–266. https://doi.org/10.1016/j.compositesb.2003.11.002

[20] Quercia, G., Chan, D., and Luke, K. (2016). Weibull statistics applied to tensile testing for oil well cement compositions. Journal of Petroleum Science and Engineering, 146, 536–544. https://doi.org/10.1016/j.petrol.2016.07.012

[21] Brandl, E., Heckenberger, U., Holzinger, V., and Buchbinder, D. (2012). Additive manufactured AlSi10Mg samples using Selective Laser Melting (SLM): Microstructure, high cycle fatigue, and fracture behavior. Materials & Design, 34, 159–169.

[22] Zhu, Z., Zhang, C., Meng, S., Shi, Z., Tao, S., and Zhu, D. (2019). A Statistical Damage Constitutive Model Based on the Weibull Distribution for Alkali-Resistant Glass Fiber Reinforced Concrete. Materials, 12, 1908. https://doi.org/doi.org/10.3390/ma12121908

[23] Weibull, W. (1951). A statistical distribution function of wide applicability. Journal of Applied Mechanics, 18, 290–293.

[24] Borzan, C. S. M., Moldovan, M., and Bocanet, V. (2018). Evaluation of Surface Modification of PA 2200 Parts Made by Selective Laser Sintering Process. Revista de Chimie, 69(4), 886–889.

[25] Chen, T., Nutter, J., Hawk, J., and Liu, X. (2014). Corrosion fatigue crack growth behavior of oil-grade nickel-base alloy 718. Part 1: effect of corrosive environment. Corrosion science, 89, 146–153.

[26] Buchbinder, D., Schleifenbaum, H., Heidrich, S., Meiners, W., and Bültmann, J. (2011). High power Selective Laser Melting (HP SLM) of aluminum parts. Physics Procedia, 12(PART 1), 271–278. https://doi.org/10.1016/j.phpro.2011.03.035